Studies on woloszynskioid dinoflagellates VII. Description of Borghiella andersenii sp. nov.: light and electron microscopy and phylogeny based on LSU rDNA

Niels Daugbjerg[a], Toke Andreasen[a], Elisabeth Happel[a], Mariana S. Pandeirada[b], Gert Hansen[a], Sandra C. Craveiro[b], António J. Calado[b] & Øjvind Moestrup[a]

[a] Marine Biological Section, Department of Biology, University of Copenhagen, Universitetsparken 4, 2100 Copenhagen Ø, Denmark

[b] Department of Biology and GeoBioSciences, GeoTechnologies and GeoEngineering (GeoBioTec) Research Unit, University of Aveiro, P-3810-193 Aveiro, Portugal
Published online: 10 Nov 2014.

PLEASE SCROLL DOWN FOR ARTICLE

Taylor & Francis
Taylor & Francis Group

Studies on woloszynskioid dinoflagellates VII. Description of *Borghiella andersenii* sp. nov.: light and electron microscopy and phylogeny based on LSU rDNA

NIELS DAUGBJERG[1], TOKE ANDREASEN[1], ELISABETH HAPPEL[1], MARIANA S. PANDEIRADA[2], GERT HANSEN[1], SANDRA C. CRAVEIRO[2], ANTÓNIO J. CALADO[2] AND ØJVIND MOESTRUP[1]

[1]*Marine Biological Section, Department of Biology, University of Copenhagen, Universitetsparken 4, 2100 Copenhagen Ø, Denmark*
[2]*Department of Biology and GeoBioSciences, GeoTechnologies and GeoEngineering (GeoBioTec) Research Unit, University of Aveiro, P-3810-193 Aveiro, Portugal*

Freshwater woloszynskioid dinoflagellates were collected independently in Scotland and Portugal and found to belong to a previously unknown species of the genus *Borghiella*, here described as *B. andersenii*. The new species differs in morphology and nuclear-encoded LSU rDNA and ITS sequences from *B. dodgei* and *B. tenuissima*, the two species presently comprising the genus *Borghiella*. Unusual features of the new species were observed particularly during asexual reproduction, which took place in the motile stage – as in many other dinoflagellates – or in a so-called division cyst, recalling cell division in the family Tovelliaceae. Such diversity in cell division is rarely reported in dinoflagellates. Morphologically *Borghiella andersenii* differs from *B. tenuissima* in being only slightly compressed dorsoventrally whereas the latter species is flat. The slight compression is also visible in lateral view. *Borghiella andersenii* and *B. dodgei* are more challenging to discriminate but the apical structure complex is only half the length in *B. andersenii* compared with *B. dodgei* (3–4 vs 6 µm). This difference can only be accounted for in the scanning electron microscope. At the light microscopy level the epicone in *B. andersenii* is rounded whereas it is conical in *B. dodgei*. Sexual reproduction in *Borghiella andersenii* was homothallic by formation of planozygotes, followed by apparent resting cysts. Phylogenetic studies on woloszynskioids have recently shown that they comprise a polyphyletic assemblage, which has been divided into the three families Borghiellaceae, Tovelliaceae and Suessiaceae. New species of the three families are now being found rapidly in many parts of the world, proving that the techniques required to investigate these small, morphologically similar dinoflagellates are now in place and proving that such 'gymnodinioids' or 'woloszynskioids' comprise an often over-looked biological entity in both marine and freshwater biotopes. Based on LSU rDNA, *B. andersenii* is most closely related to *B. tenuissima*.

Key words: asexual reproduction, *Borghiella andersenii*, cysts, freshwater dinoflagellates, ITS sequences, LSU rDNA, woloszynskioids

Introduction

The vast majority of woloszynskioid dinoflagellates are found in temperate freshwater lakes (e.g. Popovský & Pfiester, 1990) but a few species are known from marine ecosystems (Siano *et al.*, 2009, Takahashi *et al.*, 2014). The woloszynskioids differ from other dinoflagellates in having a large number of polygonal plates typically arranged in latitudinal series (e.g. Lindberg *et al.*, 2005). The systematics and evolutionary history of these dinoflagellates have recently been examined in detail and they were shown to comprise a highly polyphyletic assemblage (Lindberg *et al.*, 2005, Moestrup *et al.*, 2006, 2008, 2009*a*, 2009*b*, Pandeirada *et al.*,

2014). Hence, polygonal plates in latitudinal series have evolved multiple times during the evolution of dinoflagellate lineages, and this morphological feature should not be regarded as an indicator of relationships. Following the studies conducted within the last decade, taxa with polygonal plates are now included in the three families Borghiellaceae, Tovelliaceae and Suessiaceae (synonym Symbiodiniaceae). Additional new genera and species have been described. Thus, Moestrup *et al*. (2008) erected the genus *Borghiella* Moestrup, Gert Hansen & Daugbjerg that currently holds two species, *B. dodgei* Moestrup, Gert Hansen & Daugbjerg (the type) and *B. tenuissima* (Lauterborn) Moestrup, Gert Hansen & Daugbjerg (previously known as *Woloszynskia tenuissima* (Lauterborn) R.H. Thompson). Species of *Borghiella* belong to Group III

Correspondence to: Niels Daugbjerg.
E-mail: n.daugbjerg@bio.ku.dk

sensu Lindberg *et al.* (2005) and are characterized by a special type of apical structure complex that extends across the anterior end of the cell (Moestrup *et al.*, 2008). This system was shown to consist of a pair of narrow elongated amphiesmal vesicles (PEV). One vesicle forms a true furrow (i.e. a concave amphiesmal vesicle) while the adjoining vesicle possesses a line of knobs, apparently representing pores through which thin threads of mucilage are extruded. These vesicular rows are supported within the cell by *c.* 5 microtubules. The length of the PEV varies between the two currently known species of *Borghiella*. In *B. tenuissima* it measures *c.* 3.5 μm whereas it is 5–7 μm long in *B. dodgei*. Scanning electron microscopy has further revealed that the PEV is lined on both sides by 2 polygonal plates in *B. tenuissima* and 3–4 polygonal plates in *B. dodgei*. This apical structure complex was considered a synapomorphic feature of *Borghiella* as the closely related *Baldinia anauniensis* Gert Hansen & Daugbjerg lacked it completely (Hansen *et al.*, 2007). A relationship between *Borghiella* and *Baldinia* based on analysis of nuclear-encoded LSU rDNA sequences was also supported morphologically by the shared presence of a unique type of eyespot. This type of eyespot was designated type B by Moestrup & Daugbjerg (2007) and is characterized by a single layer of brick-like units sandwiched between a row of osmiophilic globules inside a chloroplast lobe and the sulcal amphiesmal plates.

Despite substantial differences in morphology and biogeography between the strains of *B. tenuissima* and *B. dodgei* examined (e.g. the disc-like cell shape and the incomplete cingulum in *B. tenuissima*), determination of LSU rDNA sequences has revealed a divergence of only 1.1% (pairwise comparison based on 1377 base pairs including the highly divergent domain D2; Moestrup *et al.*, 2008).

In the present study we describe the third freshwater dinoflagellate assigned to *Borghiella*, which we propose to name *B. andersenii* sp. nov. The material was collected in Scotland (2006) and Portugal (2010) and the description below is based on live material of both vegetative and cyst stages. The description includes light, scanning and transmission electron microscopy. To infer the phylogeny of *B. andersenii* we determined partial LSU rDNA sequences. To further compare the divergence at the molecular level between species of *Borghiella* we included ITS1 and ITS2 sequence data for the three known species of *Borghiella*.

Materials and methods

Cultures.　See Fig. 1 for sampling locations. The Scottish material was collected in a small pond at Ellenabeich near Oban by Robert A. Andersen (April 2006) while the Portuguese material was sampled in a flooded stream area in Ribeiro da Palha, Nariz, Aveiro (November 2010) by MP, SC and AC. A clonal culture from Scotland is maintained in the Scandinavian Culture Collection of Algae and Protozoa (SCCAP) at the University of Copenhagen as strain number
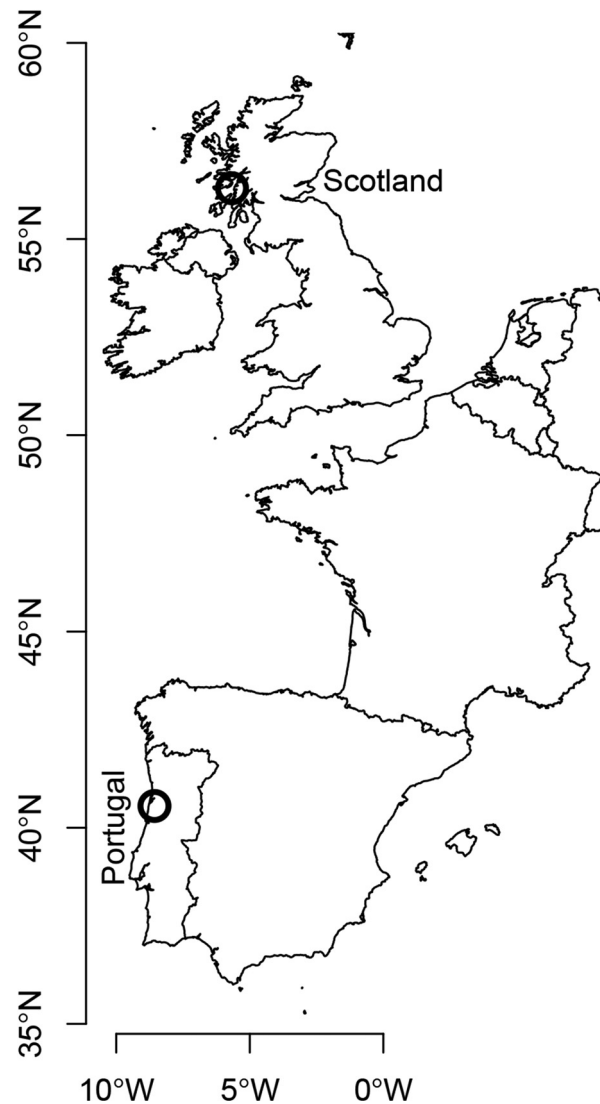
Fig. 1. Map showing locations in Scotland and Portugal, respectively, where *Borghiella andersenii* sp. nov. was sampled.

K-1120. It was grown in slightly modified MWC medium (Guillard & Lorenzen, 1972), the differences being addition of selenium and use of TES- instead of TRIS buffer (see http://www.sccap.dk/media/). Temperature was 15ºC and photoperiod 16:8 h light:dark. The culture from Portugal was grown in L16 medium (Lindström, 1991) supplemented with vitamins, at 18ºC under a 12:12 h light:dark photoperiod.

Light microscopy.　For light microscopy of living cells we used a Zeiss Axio Imager.M2 with an AxioCam HR camera (Figs 2–4), an Olympus BX51 with a Canon EOS 5D Mark II camera (Figs 5–8), and a Zeiss Axioplan 2 with a ColorView IIIu camera (Figs 17–18). Figures 11–16 were prepared from still frames from a video recording made with a JVC TK-C1481BEG colour video camera on a Leitz Biomed.

Epifluorescence microscopy.　Chloroplast morphology was studied under an inverted Olympus IX81 light microscope equipped with epifluorescence illumination and a disc-spinning unit. Micrographs were taken using a F-View *II* b/w
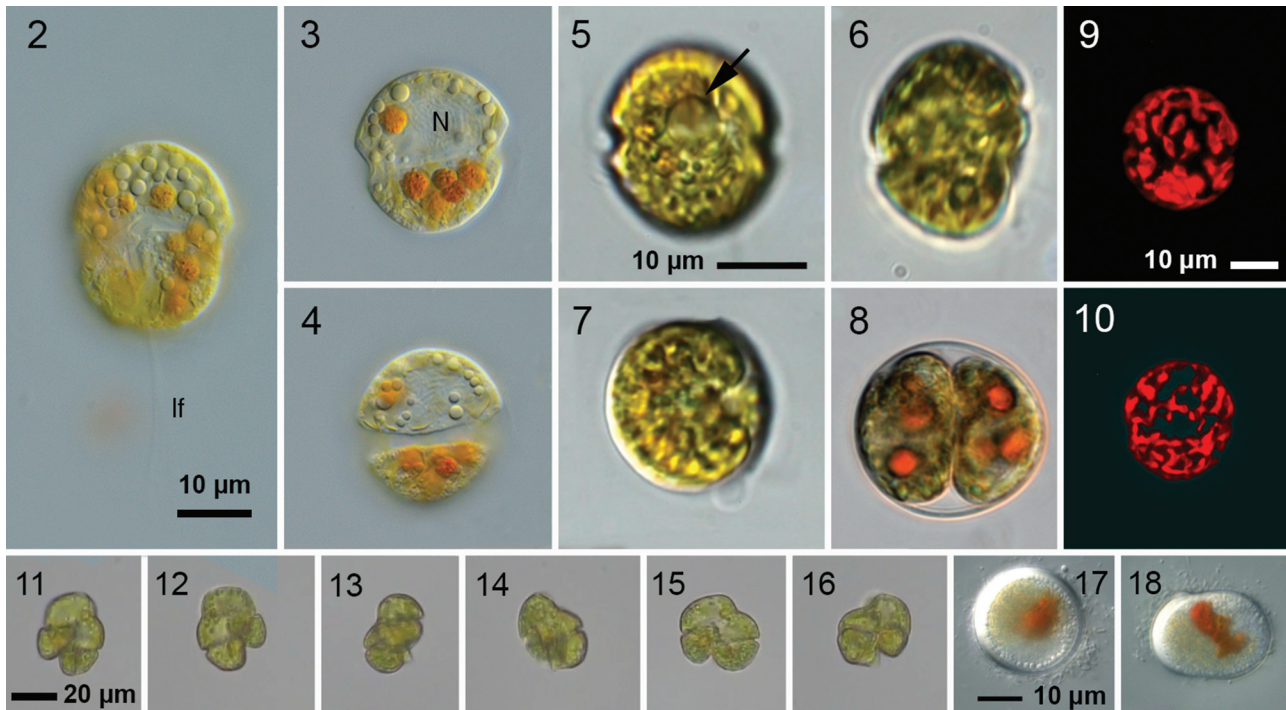
Figs 2–18. Light micrographs of *Borghiella andersenii* sp. nov. Figs 2–10: material from Scotland and Figs 11–18: material from Portugal. **Fig. 2.** Ventral view showing ventral ridge and longitudinal flagellum. **Fig. 3.** Mid focal view showing slightly wider epicone and nucleus (N) in the upper part of the cell. **Fig. 4.** Dorsal view illustrating almost equal size of epi- and hypocone. **Fig. 5.** Mid focal view showing large pusule-like vesicle (arrow) in lower part of epicone. **Fig. 6.** Left side (lateral) view with slight dorsoventral flattening especially of the hypocone. **Fig. 7.** Antapical view of sulcus, which widens posteriorly into a concave area. **Fig. 8.** Non-motile stage showing divided cell. Division cyst containing 2 daughter cells. **Figs 9–10.** Chloroplast profiles in epifluorescence microscopy showing reticulate network. **Figs 11–16.** Frame-grabbed images of video recording showing division of motile stage by fission. **Figs 17–18.** Inferred spherical and oval resting cysts (hypnozygotes) with large accumulation bodies. Note heterotrophic bacteria near the cysts.

camera (Figs 9–10) (Soft Imaging System GmbH, Münster, Germany).

Scanning electron microscopy. The fixation schedule for SEM of the Scottish material involved 300 µl of cultured material fixed in 60 µl OsO$_4$ (4%) with the addition of 60 µl distilled water and 40 µl saturated mercuric chloride (HgCl$_2$). After 15 min, cells were placed on a poly-L-lysine-coated circular coverslip and washed in distilled water for 35 min. The coverslips were dehydrated in an ethanol series (30%, 50%, 70%, 90% and 100%), then critical-point dried via liquid CO$_2$ in a BAL-TEC CPD 030 Critical Point Dryer (Bal-tec, Balzers, Liechtenstein). The coverslips were finally glued to SEM stubs with double-sided adhesive carbon tape, sputter-coated with palladium-platinum and examined in a JSM-6335F field emission scanning microscope (Jeol Ltd, Tokyo, Japan) at the University of Copenhagen. The fixation schedule for the Portuguese material involved 1 ml of culture to 1 ml of a mixture consisting of 1 part saturated HgCl$_2$ and 5 parts 2% OsO4. Cells were fixed for 15 min, collected onto 8-µm Isopore polycarbonate filters, dehydrated in an ethanol series and finally critical-point dried. Filters were sputter-coated with gold-palladium and examined with Hitachi S-4100 (Hitachi, Japan) or Jeol JSM 5400 scanning electron microscopes (Jeol Ltd, Tokyo, Japan) at the University of Aveiro.

Transmission electron microscopy. For TEM a total volume of 12 ml of the clonal culture from Scotland was mixed with 12 ml 4% glutaraldehyde in 0.2 M phosphate buffer (pH 7.8). The mixture was left for 1 h at 4ºC and then centrifuged at 2200 rpm for 10 min. The supernatant was discarded and the pellet of cells was rinsed 3 times in 0.2 M phosphate buffer at 30 min intervals at 4ºC. Post-osmication was in 1% OsO$_4$ for 1 h at 4ºC. The fixed material was then rinsed briefly in buffer and placed in an alcohol series of increasing concentrations (30%, 50%, 70% and 90%), 20 min in each rinse. It was finally placed in absolute alcohol (2 rinses, each lasting 15 min). All treatments following dehydration in 90% ethanol were conducted at room temperature. Dehydration was completed in propylene oxide (2 rinses of 5 min each). Cells were left overnight in a 1:1 mixture of propylene oxide and Spurr's resin for evaporation of the propylene oxide. Embedding was in Spurr's resin by transferring pelleted cells to an embedding dish filled with Spurr's resin. The embedding dish was placed in a 70ºC oven overnight. Thin sections were cut using a diamond knife mounted on a Leica, Super Nova, Reichert-Jung. The sections had a thickness of 50–60 nm and were collected on slot grids. They were stained for 10 min in 2% uranyl acetate at 70ºC, rinsed and stained for 10 min in Reynold's lead citrate. Examination of the sections was conducted on a JEM-1010 electron microscope (Jeol Ltd, Tokyo, Japan) at the University of Copenhagen. Micrographs were taken using a GATAN Orius SC1000 digital camera (Pleasanton, CA, USA).

DNA extraction, PCR amplification and purification of LSU rDNA. Material from Scotland: Live cells from a

clonal culture (10 ml) were harvested by centrifugation at 1200 g for 10 min. Most of the supernatant was discarded and the pellet of cells was re-suspended in *c.* 100 μl medium. Following a freezing period at −18ºC for 2 days, total genomic DNA was extracted using the cetyltrimethylammonium-bromide (CTAB) method (Doyle & Doyle, 1987) with a few modifications as described in Daugbjerg *et al*. (1994). PCR amplification and purification of partial LSU rDNA (*c.* 1500 base pairs) was conducted as outlined in Hansen & Daugbjerg (2011). Material from Portugal: Single cells of MSP8 were isolated with a micropipette under an inverted microscope and transferred to 0.2-μl PCR tubes. Following freezing at −8ºC for 3 days, *c.* 1500 base pairs of LSU rDNA were amplified with primers D1F (Scholin *et al*., 1994) and 28-1483R (Daugbjerg *et al*., 2000). The amplification kit used was illustra puReTaq Ready-To-Go PCR beads (GE Healthcare UK Ltd). The temperature for PCR amplification was similar to that in Moestrup *et al*. (2008). Amplified fragments were purified using the QIAquick PCR purification kit (Qiagen) following the manufacturer's recommendations.

PCR amplification and purification of ITS. Extracted DNA of the Scottish material of *B. andersenii* and previously extracted DNA from *B. tenuissima* and *B. dodgei* were used to amplify internal transcribed spacers 1 and 2 from the *Borghiella* species. The PCR conditions were 1 cycle at 98ºC for 2 min, followed by 35 cycles, each consisting of denaturing at 98ºC for 10 s, annealing at 60ºC for 20 s and extension at 72ºC for 30 s. A final extension step was run for 1 min at 72ºC. All PCR amplifications used the EmeraldAmp GT PCR Master Mix following the manufacturer's recommendations (TaKaRa BIO Inc, Shiga, Japan). The expected length of DNA fragments was confirmed by electrophoresis using 1.5% agarose gels run for 20 min at 150 V. DNA fragments loaded into the gel were stained with GelRed. PCR fragments were viewed using a gel documentation XR + System from BioRad (CA, USA). Fragment lengths were compared with those of a DNA marker (100 bp RAINBOW eXtended DNA ladder, BIORON GmbH, Ludwigshafen, Germany). PCR products were purified using the NucleoFast 96 PCR kit from Macherey-Nagel (GmbH & Co. KG, Düren, Germany), following the manufacturer's recommendations.

Sequence determination of LSU rDNA and ITS. Final concentrations of 500 ng of PCR fragments from LSU rDNA and ITS amplifications, respectively, were air dried and sent to Macrogen for sequence determination in both directions. We used external (D1F and 28ND-1483R) and internal primers (D2CR, D3A, D3B) for LSU rDNA sequence determination of both Scottish and Portuguese material (Hansen *et al*., 2000). It should be noted that the LSU rDNA sequences from the Scottish and Portuguese strains of *B. andersenii* were 100% identical. Thus only one, from the Scottish material, was included in the phylogenetic reconstruction (Fig. 41). For sequencing of ITS, we used ITS1 and ITS4 primers (White *et al*., 1990).

Sequence alignment and phylogenetic analyses. Information from the secondary structure of the LSU rRNA molecule was used to optimize the alignment of the dinoflagellate gene sequence, using the available data at the rRNA www server (de Rijk *et al*., 2000). The data matrix comprised 1080 base pairs (including introduced gaps). Due to its high divergence values, domain D2 was deleted prior to phylogenetic analysis. Phylogeny inference was conducted using Bayesian (BA) and maximum likelihood (ML) analyses. For BA we used MrBayes (ver. 3.2.2 x64, Ronquist & Huelsenbeck, 2003) and for ML PhyML (ver. 3.0, Guindon & Gascuel, 2003). In BA we used 20×10^6 generations, and a tree was sampled every 1000 generations. The BA analysis was run on a local computer. In order to evaluate the burn-in value we plotted the LnL values as a function of generations on a spreadsheet. The burn-in occurred after 501 000 generations (very conservative value), thus 501 trees were removed leaving 19 500 trees for generating 50% majority-rule consensus in PAUP* (Swofford, 2003). For ML analysis we applied the parameter settings obtained from jModelTest (ver. 2.1.3, Darriba *et al*., 2012). Among 88 models examined jModelTest chose GTR+I+G as the best-fit model for our data matrix with gamma = 0.658 and p-invar = 0.332. PhyML was run via the online version available on the Montpellier bioinformatics platform at http://www.atgc-montpellier.fr/phyml. The robustness of the tree topologies was evaluated using bootstrapping with 1000 replications.

Outgroup. Based on previous phylogenetic analyses using ciliates, apicomplexans and a perkinsid as outgroup taxa the dinoflagellate *Moestrupia oblonga* had the deepest divergence (see e.g. Hansen & Daugbjerg 2011). Hence, we used *Moestrupia* to polarize the other species of dinoflagellates included in this study.

Sequence divergence of ITS1 and ITS2. We used PAUP* (ver. 4b10) to calculate the sequence divergence between the three species of *Borghiella*.

Results

Borghiella andersenii *Daugbjerg, Andreasen, Happel, Pandeirada, Hansen, Craveiro, Calado & Moestrup, sp. nov.*

Description. Vegetative cells spherical and somewhat compressed dorsoventrally. Cingulum descending, displaced approximately one cingulum width. Epi- and hypocone rounded but epicone slightly wider just above the cingulum. Hypocone slightly more flattened than the epicone. Sulcus widening posteriorly into a concave area, covered in its upper part by a ventral ridge. Live cells from Scotland and Portugal similar in size: 19.9 ± 1.8 μm in length (n = 30), 15.1 ± 1.7 μm in width (n = 30) and 13.4 ± 1.9 μm in thickness (n = 12). Eyespot of type B *sensu* Moestrup & Daugbjerg (2007) but not easily seen in LM. With many yellowish-green chloroplasts, disposed at the cell periphery. Nucleus central and extending into the epicone. A narrow pair of elongate anterior amphiesmal vesicles *c.* 3–4 μm long, lined by 2–3 vesicles on each side. Asexual reproduction occurring both in the motile stage by fission and in the non-motile stage in division cysts. Sexual reproduction by formation of planozygotes with two longitudinal flagella. Size of planozygotes: 23.2 ± 0.8 μm long and 19.8 ± 1.8 μm wide (n = 4). Spherical to

elongate resting cysts with smooth wall and reddish-brown accumulation bodies.

Holotype. A fixed sample of culture K-1120 embedded in Spurr's resin has been deposited at the Botanical Museum, University of Copenhagen and serves as type material. It was given the reference number C-A-92066.

*Type locality.* Ellenabeich, a small pond near Oban, Scotland (lat. 56°17′39″N, long. 5°39′58″W).

Etymology. Species epithet *andersenii* after Dr Robert A. Andersen. Named in recognition of his many years as director of the Provasoli-Guillard National Center for the Culture of Marine Phytoplankton and for his contributions to flagellate research.

Motile cells, general morphology. Motile cells as viewed under the light microscope are illustrated in Figs 2–16. They swim rapidly and continuously in an almost straight path but after 20–30 min of observation they stop and discard their flagella (Figs 3–7). Live cells isolated from Scotland and Portugal had the same dimensions, measuring 19.9 ± 1.8 µm in length (range 17–24 µm; n = 30), 15.1 ± 1.7 µm in width (range 12–20 µm; n = 30) (widest part of cell just above the cingulum; Fig. 3). Cells were 13.4 ± 1.9 µm thick (range 11.7–17.9 µm) (n = 12). Hence, cells were slightly dorsoventrally compressed (Fig. 23), more so in the hypocone than in the epicone (see left view in Fig. 6 and antapical view in Fig. 7, Figs 22, 25). The epi- and hypocone were separated by the cingulum into two almost equal parts (Figs 2–5, 21, 24). The cingulum was displaced by one cingulum width (Figs 2, 21). The ventral ridge, behind which the transverse and longitudinal flagella emerge, can be seen in Figs 2, 21–23. The sulcus widened posteriorly into a concave area (Figs 7, 21–22 and 25). The chloroplast colour was yellowish-green. The exact number of chloroplasts was difficult to determine and they appeared to form a reticulate network as shown by epifluorescence microscopy (Figs 9–10). The chloroplast profiles were generally situated in the perimeter of the cell. The eyespot was difficult to detect in the light microscope. Large red-coloured droplets were scattered around the cell body, measuring 3–4 µm in diameter (Figs 2–4). Numerous smaller droplets (1–3 µm in diameter) were also present in the cytoplasm, most likely lipid or starch reserves (Figs 2–4). Most of the nucleus was positioned in the central part of the cell but it also reached into the upper part of the epicone (Figs 3, 29). A large pusule-like vesicle was noted in the lower part of the epicone (Fig. 5).

Asexual and sexual reproduction. During light microscopic observations, cells were found to divide both in the motile and non-motile stage. Motile cells divided obliquely by fission during swimming (Figs 11–16) and were often seen in advanced stages of division with two daughter cells already identifiable (Figs 15–16). Closer to completion of cytokinesis daughter cells were typically connected by their epicones with the upper cell almost horizontally positioned over the lower one (Fig. 19). Division of non-motile stages was often seen as two cells inside a vesicle resembling a temporary or division cyst (Fig. 8). Four cells inside a vesicle were rarely seen (not shown). The release of two daughter cells was observed once, after the vesicle wall broke open. The released cells immediately began swimming. Planozygotes, identified by the presence of two longitudinal flagella (Fig. 20), were observed in clonal cultures indicating that this species was able to reproduce sexually and is homothallic. Planozygotes measured 22–24 µm in length and 17–20 in width (n = 4). Cysts were also noticed, and these were almost colourless except for a few large red-coloured accumulation bodies (Figs 17–18). The spherical (diameter 22 µm) to elongate (26 µm × 18 µm) cysts had a smooth surface. They were often covered by heterotrophic bacteria (Figs 17–18). As *B. andersenii* reproduced sexually and the cysts were able to stay alive for several weeks we interpret them as resting cysts (hypnozygotes).

Amphiesma structure including apical structure complex. The cell surface was relatively smooth but with a few pores of apparently random distribution (e.g. Figs 21, 26, 28). The cell body was covered by a large number of polygonal amphiesmal vesicles containing thin plates arranged in latitudinal series (6–7 on the epicone and 4–5 on the hypocone; Figs 21–25). Most vesicles were 5- or 6-sided and measured 2–3 µm. The precingular series contained both pentagonal and nearly rectangular plates. Their lower side was parallel to the cingulum, forming a sharp and well-defined rim (Fig. 24). The cingulum comprised three series of plates (Fig. 28). The upper row had mostly pentagonal and a few almost rectangular
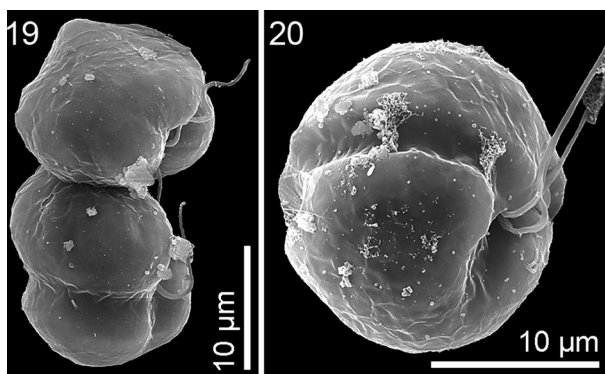
Figs 19–20. Scanning electron microscopy of *Borghiella andersenii* sp. nov. from Portugal. **Fig. 19.** Cells dividing by fission, still connected by their epicones, the upper daughter cell nearly at right angle relative to the lower one. **Fig. 20.** Planozygote with 2 longitudinal flagella.
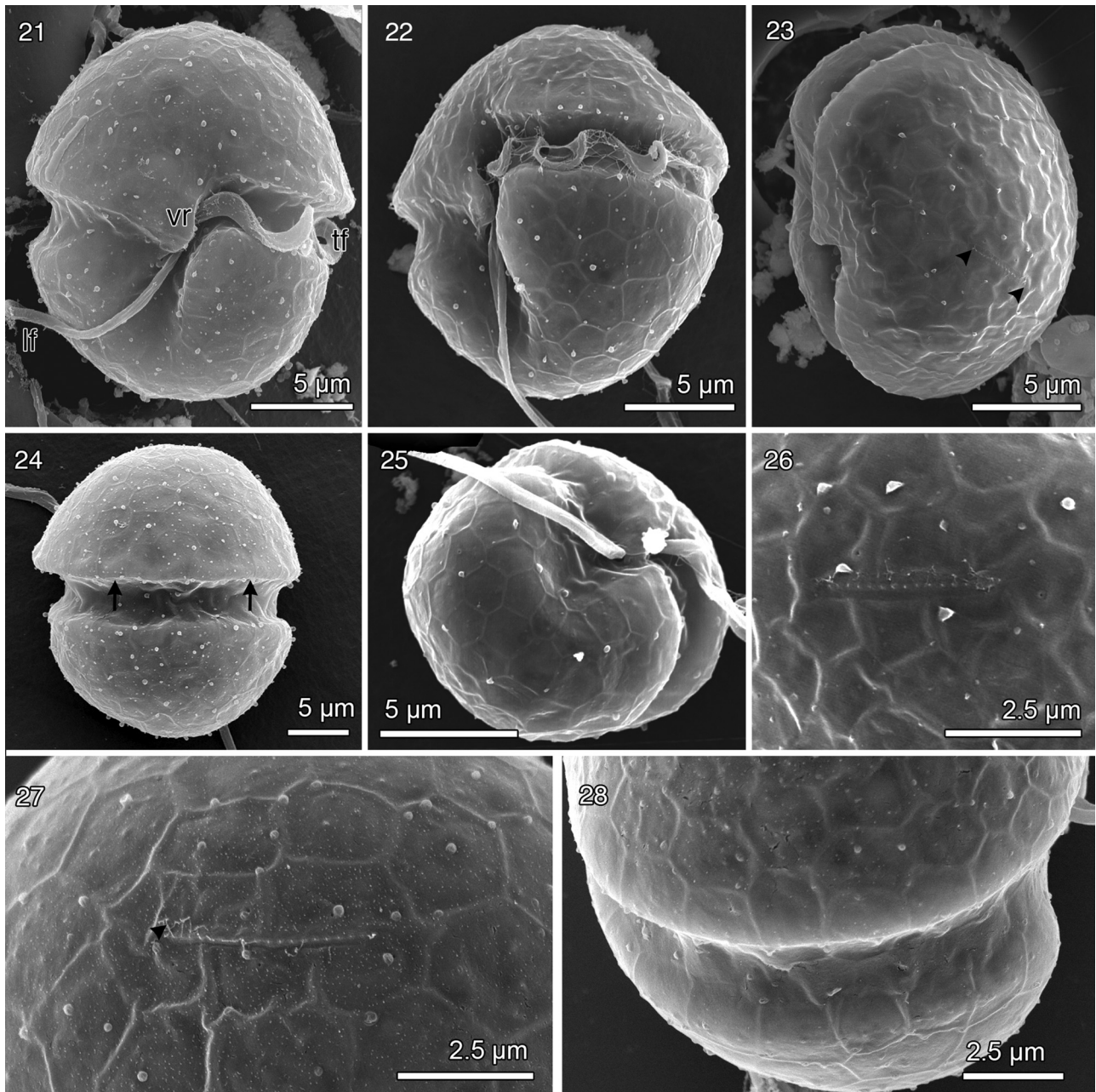
Figs 21–28. Scanning electron microscopy of vegetative cells of *Borghiella andersenii* sp. nov. (Figs 21–26: material from Portugal, Figs 27–28: material from Scotland). **Fig. 21.** Overall cell shape and plate arrangement seen in ventral view. Ventral ridge (vr) and transverse (tf) and longitudinal flagellum (lf) also visible. **Fig. 22.** Cell in ventral-left view. **Fig. 23.** Cell in apical view revealing dorsoventral compression. Notice pair of elongated amphiesmal vesicles (arrowheads indicate ends of PEV). **Fig. 24.** Dorsal view. Notice slightly wider epicone and marked transition between epicone and cingulum (arrows). **Fig. 25.** Antapical view illustrating sulcal area. **Figs 26–27.** High magnification of apical structure complex showing pairs of elongated vesicles and the adjoining thecal plates. Notice thread-like material released from axial knobs (arrowhead). **Fig. 28.** Right side view illustrating cingulum with series of plates.

plates, the middle row had mostly hexagonal and some pentagonal or rhombic plates while the posterior row comprised hexagonal plates (some nearly rectangular) that extended onto the hypocone. The ventral ridge with its S-shaped outline had a length of two amphiesmal plates and covered the flagellar pores (Figs 21–22). The apical structure complex (ASC) *sensu* Moestrup *et al*. (2014) comprised a narrow pair of straight or slightly curved, elongate amphiesmal vesicles (PEV). The length of these ranged between 1.5 and 4.5 µm but > 50% (8 out of 14 measurements) were 3.2–3.8 µm long (Figs 26, 28). The vesicle on the left side of the structure possessed 9–17 axial knobs (Figs 26, 27). Thin thread-like material was extruded through the knobs (Figs 26, 27). The PEV was lined on each side by 2–3 apical plates, either 4-, 5- or 6-sided. The elongated vesicle lying towards the right side of the cell formed a
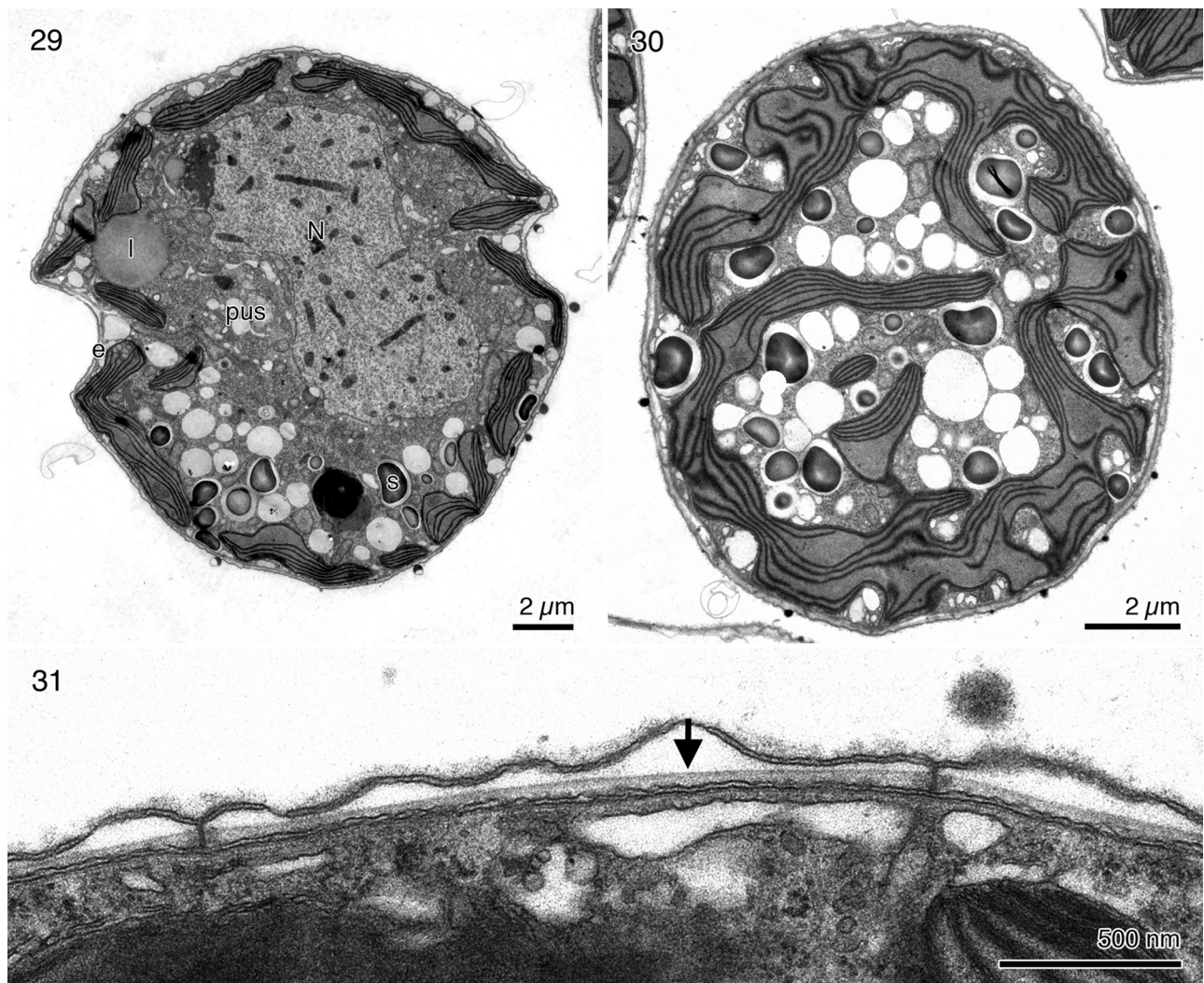
Figs 29–31. Transmission electron microscopy of *Borghiella andersenii* sp. nov. **Fig. 29.** Longitudinal section through the cell showing peripheral network of chloroplasts and centrally located nucleus (N). The figure also shows the pusular system (pus), a lipid droplet (l) the interplastidial eyespot (e), starch grains (s) and the marked anterior rim of the cingulum. **Fig. 30.** Transverse section through the hypocone to illustrate the slight dorsoventral flattening of cell. Chloroplast profiles may penetrate deep into the cell. **Fig. 31.** Section through three amphiesma vesicles each containing a thin thecal plate (arrow).

furrow (Fig. 26). The sulcal area was composed of *c.* 7, mainly hexagonal plates (Fig. 25).

Ultrastructure. Thin-sectioned material revealed the general disposition of cell organelles (Figs 29–30, 34). The somewhat wider epicone and the acute angle of the anterior, contrasting with the more open angle of the posterior part of the cingulum, are also illustrated in Fig. 29. The nucleus filled a major part of the epicone and reached slightly into the hypocone (Fig. 29). As shown in Fig. 34 it has a dorsal position. Profiles of the chloroplast(s) are best viewed in Figs 29–30. The reticulated chloroplast is positioned in the perimeter of the cell but some branches also reached deep into the cytoplasm (Fig. 30). Three membranes surround the chloroplast (Fig. 37). No pyrenoids are present. The lipid droplets and starch grains seen in the light microscope are also evident in sectioned material (Figs 29–30). This reserve material seems to be scattered

throughout the cell. The pusular system is tubular and located between the nucleus and the eyespot on the ventral side of the cell (Figs 29, 34). It opens into the canal of the transverse flagellum (Fig. 33). The cingulum is lined by 2–3 series of plates (Fig. 34). The amphiesmal vesicles contain thecal plates *c.* 50 nm thick (Fig. 31). Not all sectioned cells contained recognizable thecal plates inside amphiesmal vesicles. Instead, some vesicles contained different components (not shown) resembling those of *B. dodgei* (Moestrup *et al.* 2008, fig. 15).

Flagellar apparatus. A three-dimensional configuration of the flagellar apparatus was not aimed for in this study. However, a few details are shown in Figs 32, 33–36, 38, for comparison with the related species *B. dodgei*. The flagella are inserted at an angle somewhat wider than 90 degrees to each other (Fig. 32), the basal body of the longitudinal flagellum being inserted
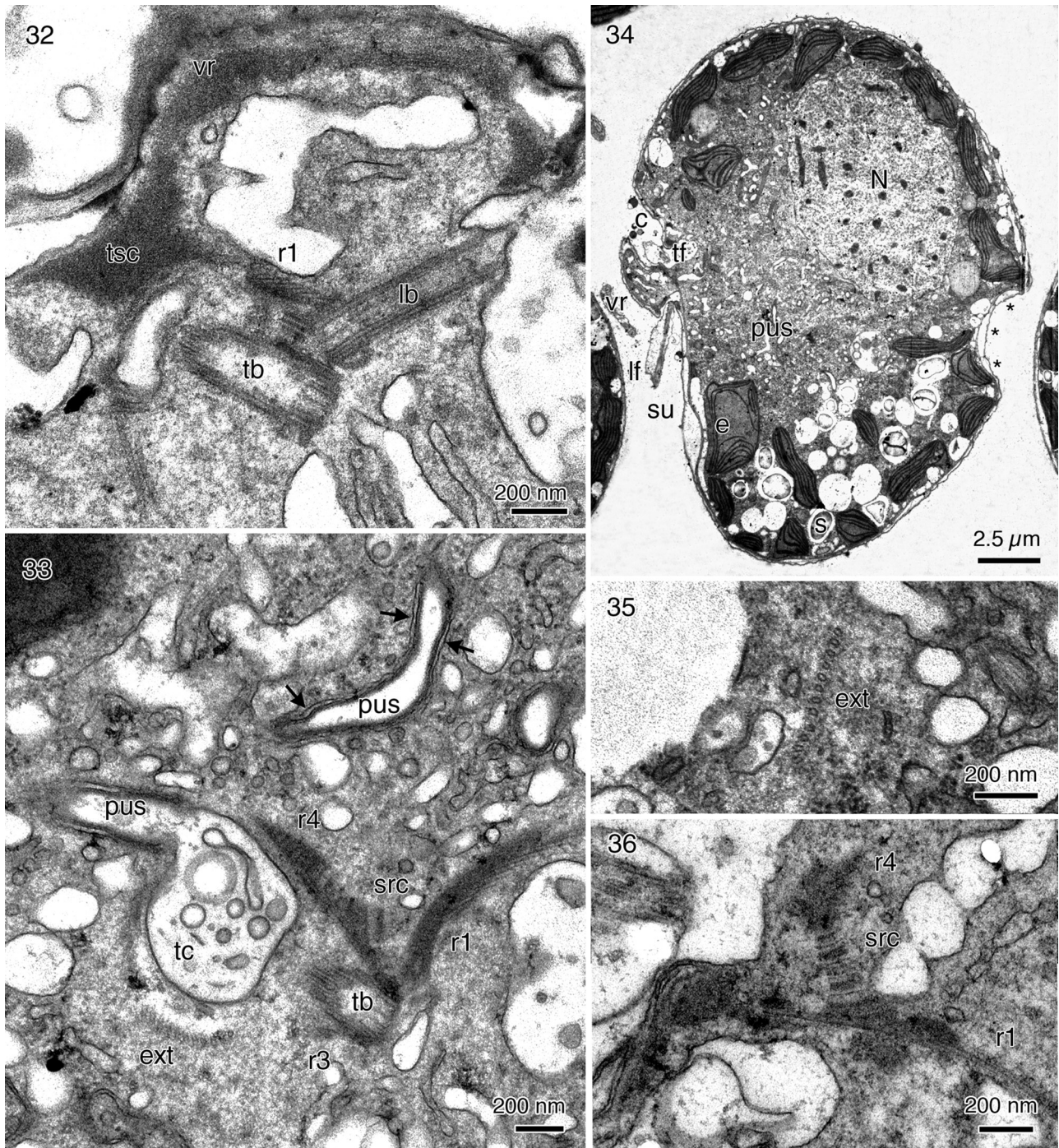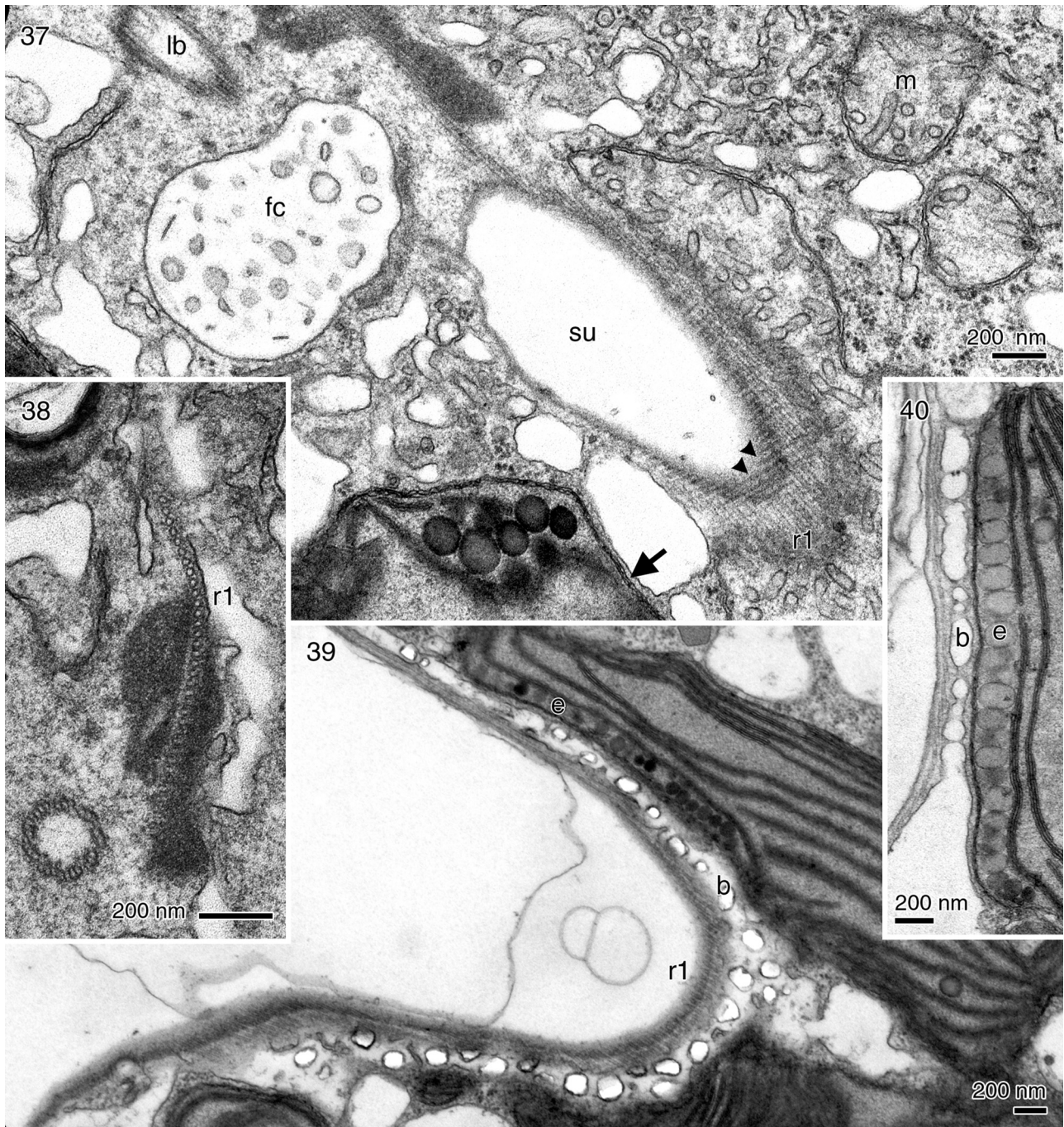
Figs 32–36. Transmission electron microscopy of *Borghiella andersenii* sp. nov. **Fig. 32.** Section through both flagellar basal bodies (longitudinal, lb and transverse, tb). Flagellar root r1 and transverse flagellum collar (tsc) also illustrated. An opaque structure connects the two collars through the ventral ridge (vr). **Fig. 33.** Section showing basal body of the transverse flagellum (tb), three microtubular roots (r1, r3, r4) and canals of the pusule system (pus), the lowermost canal emptying into the canal of the transverse flagellum (tc). The pusule system is lined by three membranes (arrows). Root r4 extends along the canal of the transverse flagellum (tc) and comprises a transversely striated component. The extension of r3 (ext) also extends along this canal. **Fig. 34.** Longitudinal section, left view illustrating marked flattening of the hypocone. Notice cingulum (c), sulcus (su), ventral ridge (vr), eyespot (e), longitudinal (lf) and transverse flagella (tf). The cingulum possesses three series of thecal plates marked by asterisks. **Fig. 35.** Microtubules forming the extension of microtubular root r3. **Fig. 36.** A conspicuous fibre (src, the striated root connective) interconnects roots r1 and r4.

on the side of the transverse flagellum basal body. Three microtubular roots were identified, all visible in Fig. 33. Root r1 is multi-stranded (Fig. 38) and associates with the basal body of the longitudinal

flagellum, while r3 and r4, which probably comprise only a single microtubule each, attach to the basal body of the transverse flagellum. In addition, r1 and r4 are attached to each other by a distinctly banded

Figs 37–40. Transmission electron microscopy of *Borghiella andersenii* sp. nov. **Fig. 37.** Tangential section of the sulcal area of the cell, showing the basal body of the longitudinal flagellum (lb) at top left, the flagellar canal (fc) below, and the sulcus (su) lined by the microtubules of r1. A system of very fine fibres (arrowheads) is located at right angle to the root microtubules. m, mitochondrion. The chloroplast is surrounded by three membranes (arrow). **Fig. 38.** The microtubular root r1 comprises many microtubules, here *c*. 30. The basal body bottom, left, is from the longitudinal flagellum. **Fig. 39.** Section through the hypocone and sulcus at some distance below the flagellar insertion area, showing eyespot (e), and single row of vacuoles with brick-like material (b). Flagellar root r1 is seen in oblique section. **Fig. 40.** Interplastidial eyespot comprising a single row of carotenoid globules. Empty-looking vacuoles are located between the chloroplast and the microtubules of root r1.

SRC ('striated root connector') (Figs 33, 36). Root r4 includes a cross-banded component (Fig. 33). Root r3 is a microtubule-nucleating root, a band of nucleated microtubules (12 in Fig. 35) extending at approximately right angles to the root and passing close to the flagellar canal of the transverse flagellum (Fig. 33). Root r1 extends along the sulcus, reaching the eyespot (Fig. 39). The band of microtubules is associated with a layer of very thin fibres, which cross the ventral surface of the microtubules at right angles (Fig. 37). The sectioned material did not reveal the presence of root r2. Both flagellar canals are surrounded near their exit point by striated collars, parts of which are visible in Fig. 32. An opaque fibre
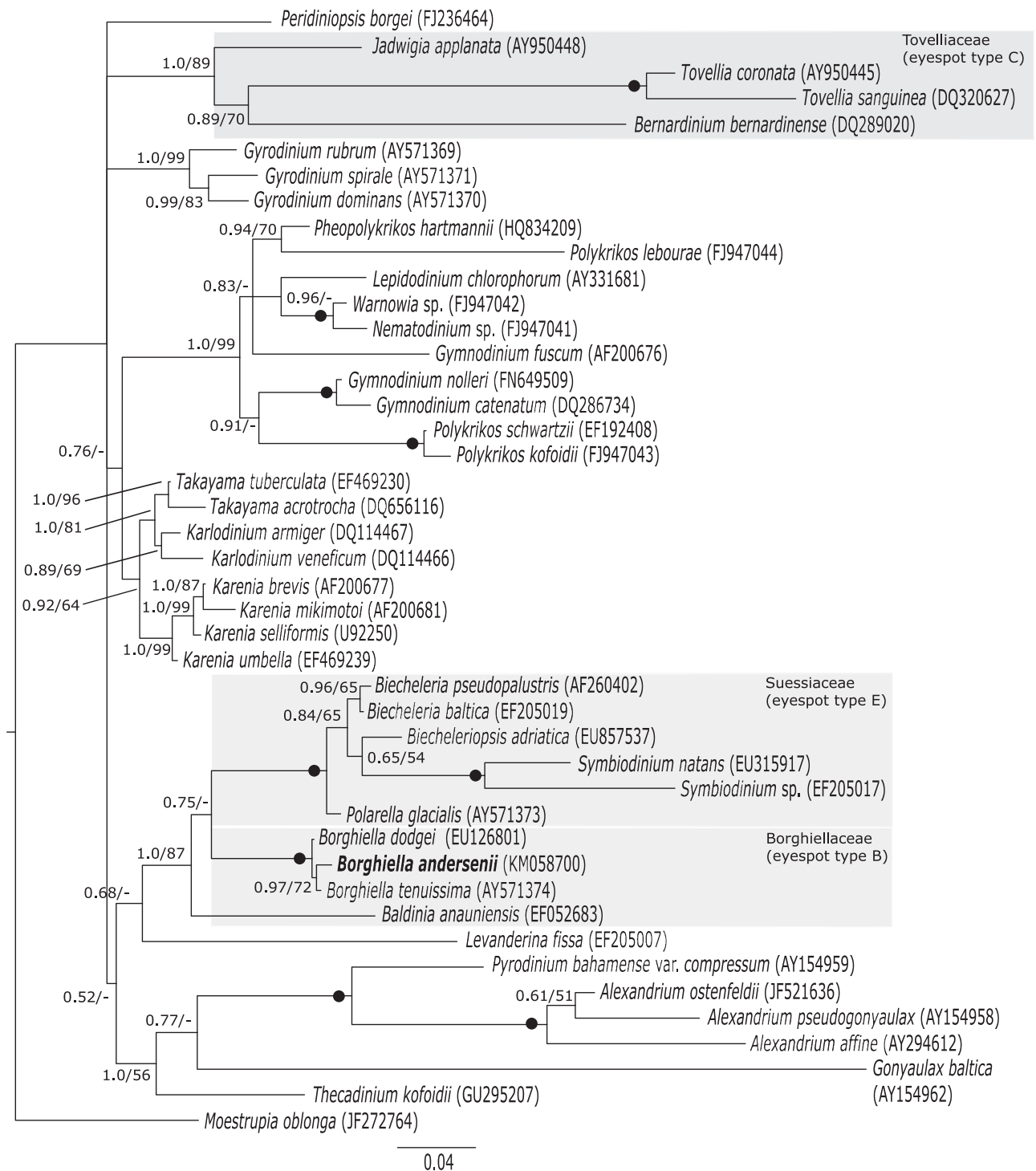
Fig. 41. Phylogeny of *Borghiella andersenii* sp. nov. from Scotland (strain K-1120) based on nuclear-encoded partial LSU rDNA (1080 base pairs) and inferred from Bayesian analysis. *Moestrupia oblonga* formed the outgroup which was used to polarize the ingroup comprising 25 other dinoflagellate genera (43 species). Posterior probabilities from Bayesian analyses and bootstrap values from maximum likelihood analyses with 1000 replications are written to the left of internodes. Bootstrap values below 50% are indicated by a '-'. GenBank accession numbers are written in parentheses following the species names. Families of woloszynskioid dinoflagellates are indicated in grey rectangles as well as their type of eyespot *sensu* Moestrup and Daugbjerg (2007). Branch lengths are proportional to the number of character changes.

extends between the collars through the ventral ridge area (Fig. 32). Canals of the pusule system are visible in Fig. 33. They appeared more or less empty, apart from occasional vesicular material. The lowermost pusule tube in Fig. 33 opens into the canal of the transverse flagellum. The three membranes lining

canals of the pusule system were often clearly visible (Fig. 33, arrows).

Eyespot. Details of the eyespot are illustrated in Figs 37, 39–40. The morphological outline matches type B *sensu* Moestrup & Daugbjerg (2007) as it comprises a

single row of carotenoid globules positioned inside a chloroplast (Fig. 40). A series of brick-like units, or sometimes empty-looking vacuoles, are located between the eyespot and the plasma membrane (Fig. 40). The flagellar root r1 lies adjacent to the brick-containing vacuoles (Fig. 39).

Molecular phylogeny. Bayesian analysis of nuclear-encoded partial LSU rDNA of 26 genera (44 species) of dinoflagellates revealed that *Borghiella andersenii* formed a sister taxon to *B. tenuissima* (pp = 0.97 and BS = 72%). These two *Borghiella* species formed a sister group to *B. dodgei* (Fig. 41). The genus *Borghiella* received maximum support by posterior probability (pp = 1.0) and bootstrap value (BS = 100%). The present phylogenetic inference did not provide support for monophyly of the family Borghiellaceae, as *Baldinia anauniensis* formed a sister taxon to *Borghiella* spp. and the family Suessiaceae. However, the sister group relationship between *Borghiella* and the six species of Suessiaceae received only little support from Bayesian analysis (pp = 0.75) and less than 50% bootstrap support indicating that they could equally well be related to *Baldinia*. Such a relationship is strongly favoured by the same morphology of the eyespot (type B, *sensu* Moestrup & Daugbjerg 2007) (Fig. 41). The two other families of woloszynskioid dinoflagellates were highly supported (Tovelliaceae, pp = 1.0 and BS = 89%; Suessiaceae, pp = 1.0 and BS = 100%).

Sequence divergence based on LSU rDNA and ITS. Estimates of sequence divergence for all pairwise comparisons are shown in Table 1. When based on partial LSU rDNA (1319 base pairs) the lowest sequence divergence was seen between *B. dodgei* and *B. tenuissima* (1.1%). The difference between *B. andersenii* and *B. tenuissima* was 1.5% whereas it was 2% between *B. andersenii* and *B. dodgei*. In general, sequence divergence estimates between *Borghiella* spp. based on LSU rDNA were low, perhaps indicating a recent splitting event.

This is in contrast to the ITS1-5.8S rDNA-ITS2 data (569 base pairs), for which the lowest divergence estimate was between *B. andersenii* and *B. dodgei* (9.3%) and the highest between *B. andersenii* and *B. tenuissima* (11.9%).

Table 1. Sequence divergence in per cent of *Borghiella* spp., calculated using the Kimura-2-parameter model. Above diagonal: Estimates of divergence based on nuclear encoded LSU rDNA (1319 base pairs). Below diagonal: Estimates of divergence based on ITS 1, 5.8S rDNA and ITS 2 (569 base pairs).

	B. andersenii	*B. tenuissima*	*B. dodgei*
B. andersenii	-	1.5	2.0
B. tenuissima	11.9	-	1.1
B. dodgei	9.2	9.3	-

Discussion

Thin-walled small dinoflagellate species are difficult to study as they offer very few morphological characters for identification. However, finding the same species in two widely separated geographic areas over 4 years apart indicates that the technical problems associated with studying these flagellates have now been overcome and that we can expect not only numerous new findings of the species known, but also that many previously undescribed species will be found. This opens up opportunities for studies on the ecology and biogeography of the different species.

Distribution of Borghiella *species.* The two *Borghiella* species (viz. *B. andersenii* and *B. dodgei*) are morphologically very similar to each other and have been found in small lakes, *B. dodgei* in the oligotrophic Lake Tovel in Northern Italy, and the Scottish and Portuguese material of *B. andersenii* from a pond and from running water, respectively. The Portuguese strain of *B. andersenii* was previously illustrated under the name *B. dodgei* by Pandeirada *et al.* (2013), who noted the different epicone shape but did not propose a new species for lack of further morphological and molecular data. The third species, *B. tenuissima*, which is readily identified because of its very flattened cells, was originally described in 1894 from the Upper Rhine river (Lauterborn, 1894) and has since been recorded in other central and north European localities e.g. Romania (Caraus, 2012) and Britain (Lewis & Dodge, 2002). More recently there have been records of the species outside Europe, from the snow-covered Lake Helen, close to Kangerlussuaq, near the border of the inland ice sheet of West Greenland (Moestrup *et al.*, 2008) and from China (Liu & Hu, 2006).

Identification of Borghiella *spp.* Table 2 compiles the most significant morphological differences between the three species of *Borghiella* based on light and electron microscopy. *Borghiella tenuissima* is a cold-water species that is unusual in having an incomplete cingulum on the ventral side of the cell and it is both longer and wider than its congeners (Table 2). It has sometimes been confused with *Tovellia leopoliensis* (Woloszyńska) Ø. Moestrup, K. Lindberg & N. Daugbjerg (e.g. Popovský & Pfiester, 1990, p. 147). The latter is also strongly flattened dorsoventrally but differs in having a complete cingulum, a different ecology and a different type of resting cyst. *Borghiella andersenii* and *B. dodgei* are morphologically much more similar in cell dimensions and outline (Figs 42–43). However, these two species can be distinguished at the light microscopic level by the shape of the epicone, which is rounded in *B. andersenii* and conical in *B. dodgei*. At the scanning electron microscopic level a few additional features distinguish the two species. The apical structure complex in *B.*

Table 2. A morphological comparison between the three species of *Borghiella* currently known (based on light and electron microscopy).

Characters	Length × width (µm)	Cell shape	Path of cingulum	Rows of plates in cingulum	Ventral part of hypocone	Apical structure complex	Shape of ventral ridge	Shape and texture of resting cyst	Reference
B. tenuissima	40 × 35	Oval, flat (leaf-like)	Incomplete	2	Flat	C. 3–4 µm long*; Surrounded by c. 7 plates*	No s- or z-shape	Globular and smooth	1, 2
B. dodgei	12–22 × 14–15	Round; epicone slightly conical-shaped, hypocone more so	Complete, displaced 1 cingulum width	2–3	Concave	C. 6 µm long; 29 knobs Surrounded by 9 plates	z-shape	?	1
B. andersenii	17–24 × 12–20	Round; epicone somewhat flattened, hypocone more so	Complete, displaced 1 cingulum width	2–3	Concave	C. 3–4 µm long; up to 17 knobs, surrounded by 8 plates	s-shape	Spherical to elongate and smooth	3

1: Moestrup *et al.*, 2008; 2: von Stosch, 1973; 3: Present study. *Estimated number based on figs 58–62 in Moestrup *et al.* (2008).
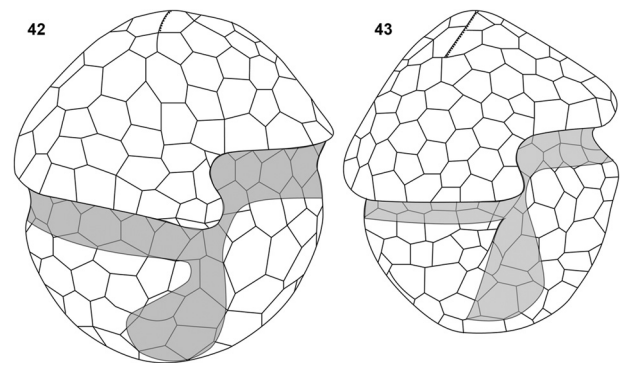
Figs 42–43. Drawings of *Borghiella andersenii* sp. nov. (Fig. 42) and *B. dodgei* (Fig. 43); not to scale. **Fig. 42.** Cell in ventral view. Cingulum and sulcus marked in grey. **Fig. 43.** Cell in ventral view. Cingulum and sulcus marked in grey.

andersenii is 3–4 µm long whereas it is twice as long in *Borghiella dodgei* (*c.* 6 µm). The shape of the ventral ridge also differs slightly (s-shaped in *B. andersenii* and z-shaped in *B. dodgei*).

Sexual and asexual reproduction. Sexual reproduction in *B. andersenii* was strongly suggested by the appearance of planozygotes in clonal cultures (Fig. 20). This indicated the occurrence of self-fertilization (homothallism). Previous references to sexual reproduction in the Borghiellaceae have been based on observations of apparent resting cysts. In the present species we also interpreted the cells shown in Figs 17–18 as resting cysts. Their appearance remained unchanged for several weeks without signs of degradation of contents. The resting cysts of *B. andersenii* were spherical to elongate in outline and with smooth walls and thus with a similar morphology to *B. tenuissima* as described by von Stosch (1973) and Moestrup *et al.* (2008). *Borghiella andersenii* is atypical in displaying two different types of cell division: (1) division in the motile stage and (2) division within the so-called division cyst. The first type is the common type in naked and some kinds of armoured dinoflagellates, from *Gymnodinium fuscum* (Ehrenberg) F. Stein (Gymnodiniales) and *Biecheleria pseudopalustris* (J. Schiller) Moestrup, K. Lindberg & Daugbjerg (Suessiales) to *Ceratium* Schrank (Gonyaulacales), while division cysts are common in the Peridiniales. Members of the family Tovelliaceae, a family of somewhat uncertain phylogenetic relationship, are characterized by cells dividing in division cysts (e.g. Wołoszyńska 1917). The cells become immotile and the contents divide into 2–8 zoospores, as in the green alga *Chlamydomonas* Ehrenberg. The finding of both types of cell division in *B. andersenii* was therefore somewhat unexpected, and had to our knowledge only previously been observed in *Gymnodinium pseudomirabile* Hansen & Flaim (Hansen & Flaim, 2007) and in the two thecate dinoflagellates *Lingulodinium polyedrum* (Figueroa & Bravo, 2005) and *Alexandrium*

peruvianum (Figueroa *et al.*, 2008). In closely related species, *B. dodgei* cell division was reported to take place by fission in the motile stage, but considering the close phylogenetic relationship between the two species, it appears likely that both types of cell division may also be found in *B. dodgei*. In *B. tenuissima* cell division in the motile stage was illustrated in a single figure by Wołoszyńska (1917, fig. 9) but not described in the text. The merit of being able to divide in different ways is not clear, and the process of cell division in dinoflagellates generally requires more detailed studies.

Sequence divergence. While *B. tenuissima* is morphologically very different from the other species of *Borghiella*, the sequence divergence between *B. tenuissima* and *B. andersenii* and *B. dodgei,* respectively, is only 1.1–1.5%. In fact *B. andersenii* and *B. dodgei*, which morphologically are much more similar to each other than either of them is to *B. tenuissima*, differ by *c.* 2% from each other. A similar discrepancy between molecular and morphological data has been reported elsewhere in dinoflagellates, most strikingly by Logares *et al.* (2007) who reported identical ribosomal sequences (SSU, ITS1, ITS2, 5.8 S, partial LSU) in *Scrippsiella hangoei* (J. Schiller) J. Larsen and *Peridinium aciculiferum* Lemmermann, despite the two species being phenotypically and ecologically distinct. Ribosomal genes of two additional species in this complex, *P. baicalense* Kisselew & Swetkow and *P. euryceps* K. Rengefors & B. Meyer are also very similar to *S. hangoei* and *P. aciculiferum* (Annenkova *et al.*, unpublished). Such non-parallel evolution of ribosomal genes and morphology is unexpected, considering the reliance given to ribosomal genes as indicators of phylogeny. We have no obvious explanation why the divergence based on ITS sequences implies a different relationship between species of *Borghiella* compared with LSU rDNA.

Acknowledgements

Funding

References

CARAUS, I. (2012). Algae of Romania. A distributional checklist of actual algae. Version 2.3 third revision. University of Bacau, Bacau.

DARRIBA, D., TABOADA, G.L., DOALLO, R. & POSADA, D. (2012). jModelTest 2: more models, new heuristics and parallel computing. *Nature Methods*, **9**: 772.

DAUGBJERG, N., MOESTRUP, Ø. & ARCTANDER, P. (1994). Phylogeny of the genus *Pyramimonas* (Prasinophyceae) inferred from the *rbc*L gene. *Journal of Phycology*, **30**: 991–999.

DAUGBJERG, N., HANSEN, G., LARSEN, J. & MOESTRUP, Ø. (2000). Phylogeny of some of the major genera of dinoflagellates based on ultrastructure and partial LSU rDNA sequence data, including the erection of three new genera of naked dinoflagellates. *Phycologia*, **39**: 302–317.

DE RIJK, P., WUYTS, J., VAN DER PEER, Y., WINKELMANS, T. & DE WACHTER, R. (2000). The European large subunit ribosomal RNA database. *Nucleic Acids Research*, **28**: 117–118.

DOYLE, J.J. & DOYLE, J.L. (1987). A rapid DNA isolation procedure for small quantities of fresh leaf tissue. *Phytochemical Bulletin*, **19**: 11–15.

FIGUEROA, R.I. & BRAVO, I. (2005). Sexual reproduction and two different encystment strategies of *Lingulodinium polyedrum* (Dinophyceae) in culture. *Journal of Phycology*, **41**: 370–379.

FIGUEROA, R.I., BRAVO, I. & GARCÉS, E. (2008). The significance of sexual versus asexual cyst formation in the life cycle of the noxious dinoflagellate *Alexandrium peruvianum*. *Harmful Algae*, **7**: 653–663.

GUILLARD, R. R. L. & LORENZEN, C. J. (1972). Yellow-green algae with chlorophyllide c. *Journal of Phycology*, **8**: 10–14.

GUINDON, S. & GASCUEL, O. (2003). A simple, fast, and accurate algorithmn to estimate large phylogenies by maximum likelihood. *Systematic Biology*, **52**: 694–704.

HANSEN, G. & DAUGBJERG, N. (2011). *Moestrupia oblonga* gen. et comb. nov. (syn.: *Gyrodinium oblongum*), a new marine dinoflagellate genus characterized by light and electron microscopy, photosynthetic pigments and LSU rDNA sequence. *Phycologia*, **50**: 583–599.

HANSEN, G. & FLAIM, G. (2007). Dinoflagellates of the Trentino Province, Italy. *Journal of Limology* 66: 107–141.

HANSEN, G., DAUGBJERG, N. & HENRIKSEN, P. (2000). Comparative study of *Gymnodinium mikimotoi* and *Gymnodinium aureolum* comb. nov (= *Gyrodinium aureolum*) based on morphology, pigment composition, and molecular data. *Journal of Phycology*, **36**: 394–410.

HANSEN, G., DAUGBJERG, N. & HENRIKSEN, P. (2007). *Baldinia anauniensis* gen. et sp. nov.: a 'new' dinoflagellate from Lake Tovel, N. Italy. *Phycologia*, **46**: 86–108.

LAUTERBORN, R. (1894). Über die Winterfauna einiger Gewässer der Oberrheinebene. *Biologisches Zentralblatt*, **14**: 390–398.

LEWIS, J.M. & DODGE, J.D. (2002). Phylum Pyrrophyta (Dinoflagellates). In *The Freshwater Algal Flora of the British Isles* (John, D.M., Whitton, B.A. & Brook, A.J., editors), 186–207. Cambridge University Press, Cambridge.

LINDBERG, K., MOESTRUP, Ø. & DAUGBJERG, N. (2005). Studies on woloszynskioid dinoflagellates I: *Woloszynskia coronata* re-examined using light and electron microscopy and partial LSU rDNA sequences, with description of *Tovellia* gen. nov and *Jadwigia* gen. nov. (Tovelliaceae fam. nov.). *Phycologia*, **44**: 416–440.

LINDSTRÖM, K. 1991. Nutrient requirements of the dinoflagellate *Peridinium gatunense*. *Journal of Phycology*, **27**: 207–219.

LIU, G. & HU, Z. (2006). Two genera of freshwater Dinophyta newly recorded from China. *Acta Phytotaxonomica Sinica*, **44**: 189–194.

LOGARES, R., RENGEFORS, K., KREMP, A., SHALCHIAN-TABRIZI, K., BOLTOVSKOY, A., TENGS, T., SHURTLEFF, A. & KLAVENESS, D. (2007). Phenotypically different microalgal morphospecies with identical ribosomal DNA: a case of rapid adaptive evolution? *Microbial Ecology*, **53**: 549–561.

MOESTRUP, Ø. & DAUGBJERG, N. (2007). On dinoflagellate phylogeny and classification. In *Unravelling the Algae: The Past, Present, and Future of Algae Systematics* (Brodie, J. & Lewis, J., editors), Systematics Association Special Volumes, vol. 75, pp. 215–230. CRC Press, Boca Raton, FL.

MOESTRUP, Ø., HANSEN, G., DAUGBJERG, N., FLAIM, G. & D'ANDREA, M. (2006). Studies on woloszynskioid dinoflagellates II: On

Tovellia sanguinea sp. nov., the dinoflagellate species responsible for the reddening of Lake Tovel, N. Italy. *European Journal of Phycology*, **41**: 47–65.

MOESTRUP, Ø., HANSEN, G. & DAUGBJERG, N. (2008). Studies on woloszynskioid dinoflagellates III: On *Borghiella* gen. nov., and *B. dodgei* sp. nov., a cold-water species from Lake Tovel, N. Italy, and on *B. tenuissima* comb. nov. (syn. *Woloszynskia tenuissima*). *Phycologia*, **47**: 54–78.

MOESTRUP, Ø., LINDBERG, K. & DAUGBJERG, N. (2009a). Studies on woloszynskioid dinoflagellates IV: the genus *Biecheleria* gen. nov. *Phycological Research*, **57**: 203–220.

MOESTRUP, Ø., LINDBERG, K. & DAUGBJERG, N. (2009b). Studies on woloszynskioid dinoflagellates V. Ultrastructure of *Biecheleriopsis* gen. nov., based on investigations of *B. adriatica* (Lebour) comb. nov. (syn. *Gymnodinium pygmaeum* Lebour). *Phycological Research*, **57**: 221–237.

MOESTRUP, Ø., HAKANEN, P., HANSEN, G., DAUGBJERG, N. & ELLEGAARD, M. (2014). On *Levanderina fissa* gen. et comb. nov. (Dinophyceae) (syn. *Gymnodinium fissum, Gyrodinium instriatum, G. uncatenum)*, a dinoflagellate with a very unusual sulcus. *Phycologia*, **53**: 265–292.

PANDEIRADA, M.S., CRAVEIRO, S.C. & CALADO, A.J. (2013). Freshwater dinoflagellates in Portugal (W Iberia): a critical checklist and new observations. *Nova Hedwigia*, **97**: 321–348.

PANDEIRADA, M.S., CRAVEIRO, S.C., DAUGBJERG, N., MOESTRUP, Ø. & CALADO, A.J. (2014). Studies on woloszynskioid dinoflagellates VI: description of *Tovellia aveirensis* sp. nov. (Dinophyceae), a new species of Tovelliaceae with spiny cysts. *European Journal of Phycology*, **49**: 230–243.

POPOVSKÝ, J. & PFIESTER, L.A. (1990). Süßwasserflora von Mitteleuropa. Vol. 6. *Dinophyceae (Dinoflagellida)*, pp. 272. Gustav Fischer, Jena.

RONQUIST, F. & HUELSENBECK J.P. (2003). MrBayes 3: Bayesian phylogenetic inference under mixed models. *Bioinformatics*, **19**: 1572–1574.

SCHOLIN, C.A., HERZOG, M., SOGIN, M. & ANDERSON, D.M. (1994). Identification of group- and strain-specific genetic markers for globally distributed *Alexandrium* (Dinophyceae). II. Sequence analysis of a fragment of the LSU rRNA gene. *Journal of Phycology*, **30**: 999–1011.

SIANO, R., KOOISTRA, W.H.C.F., MONTRESOR, M. & ZINGONE, A. (2009). Unarmoured and thin-walled dinoflagellates from the Gulf of Naples, with the description of *Woloszynskia cincta* sp. nov. (Dinophyceae, Suessiales). *Phycologia*, **48**: 44–65.

SWOFFORD, D.L. (2003). *PAUP* Phylogenetic Analysis using Parsimony (*and other Methods), Version 4*. Sinauer Associates, Sunderland, MA.

TAKAHASHI, K., SARAI, C. & IWATAKI, M. (2014). Morphology of two marine woloszynskioid dinoflagellates, *Biecheleria brevisulcata* sp. nov. and *Biecheleriopsis adriatica* (Suessiaceae, Dinophyceae), from Japanese coasts. *Phycologia*, **53**: 52–65.

VON STOSCH, H.A. (1973). Observations on vegetative reproduction and sexual life-cycles of two freshwater dinoflagellates, *Gymnodinium pseudopalustre* Schiller and *Woloszynskia apiculata* sp. nov. *Brittish Phycological Journal*, **8**: 105–134.

WHITE, T.J., BRUNS, T., LEE, S. & TAYLOR, J.W. (1990). Amplification and direct sequencing of fungal ribosomal RNA genes for phylogenetics. In *PCR Protocols: A Guide to Methods and Applications* (Innis, M.A., Gelfand, D.H., Sninsky, J.J. & White, T.J. (editors), 315–322. Academic Press, New York.

WOŁOSZYŃSKA, J. (1917). Neue Peridineen-Arten, nebst Bemerkungen über den Bau der Hülle bei *Gymno-* und *Glenodinium. Bulletin International de l'Academie des Sciences de Cracovie, Classe des Sciences Mathématiques et Naturelles, série B: Sciences Naturelles*, **1917**: 114–122, pls 11–13.